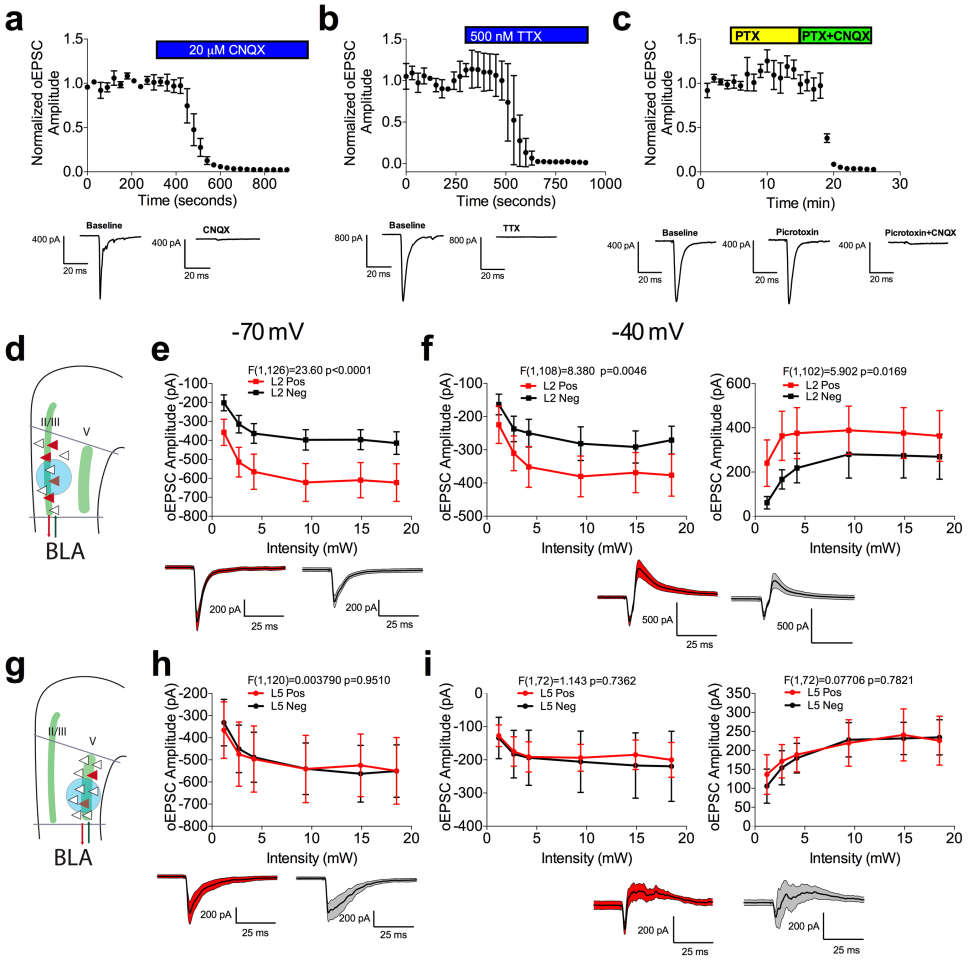

Figure S1, related to figure 2: Stimulation of BLA terminals in the plPFC elicits a monosynaptic excitatory and disynaptic inhibitory current

(a) Effect of the AMPAR antagonist CNQX (20 μM) on oEPSC amplitude at BLA-plPFC synapses. Bath application of CNQX abolished oEPSCs (n=3, N=2).

(b) Effect of the Voltage Gated Sodium Channel blocker Tetrodotoxin (TTX)(500nM) on oEPSC amplitude at BLA-plPFC synapses. Bath application of TTX abolished oEPSCs (n=3, N=2).

(c) Effect of the $GABA_AR$ channel blocker picrotoxin (PTX)(50 μM) on oEPSC amplitude at BLA-plPFC synapses. Bath application of PTX did not affect oEPSCs, while subsequent addition of CNQX abolished oEPSCs (n=3, N=2).

(d) Schematic for voltage-clamp recordings of oEPSCs from L2/3 rAAV-positive (rAAV+) and rAAV-negative (rAAV-) neurons at -70mV (left) and -40mV (right).

(e) Optically evoked input/output curve from L2/3 rAAV+ and rAAV- neurons at -70mV. The BLA sends stronger excitatory input to reciprocally projecting L2/3 neurons (n=11, N=5) than non-reciprocally projecting neurons L2/3 neurons (n=12, N=5)

(f) Optically evoked input/output curve from L2/3 rAAV+ and negative neurons at -40mV. Stimulation of BLA terminals in the plPFC elicits a monosynaptic excitatory and disynaptic inhibitory current, presumably through feed-forward inhibition. Both

excitatory and inhibitory responses are larger in L2/3 rAAV+ neurons (n=10, N=5) compared to rAAV- neurons at -40mV (n=9, N=5).

(g) Schematic for voltage-clamp recordings of oEPSCs from L2/3 rAAV+ and rAAV- neurons at -70mV (left) and -40mV (right).

(h) Optically evoked input/output curve from L5 rAAV+ and rAAV- neurons at -70mV. No difference in excitatory input to L5 rAAV+ (n=11 ,N=5) compared to rAAV- neurons (n=11, N=5) was observed.

(i) Optically evoked input/output curve from L5 rAAV+ and rAAV- neurons at -40mV. Stimulation of BLA terminals in the plPFC elicited a monosynaptic excitatory and disynaptic inhibitory current. No difference in excitatory or inhibitory response in L5 rAAV+ (n=7, N=5) compared to rAAV- neurons at -40mV was observed (n=7, N=5).

All error bars represent ± SEM. "n" represents number of neurons, "N" represents number of mice. F and P values from 2-way ANOVA shown in relevant panels.

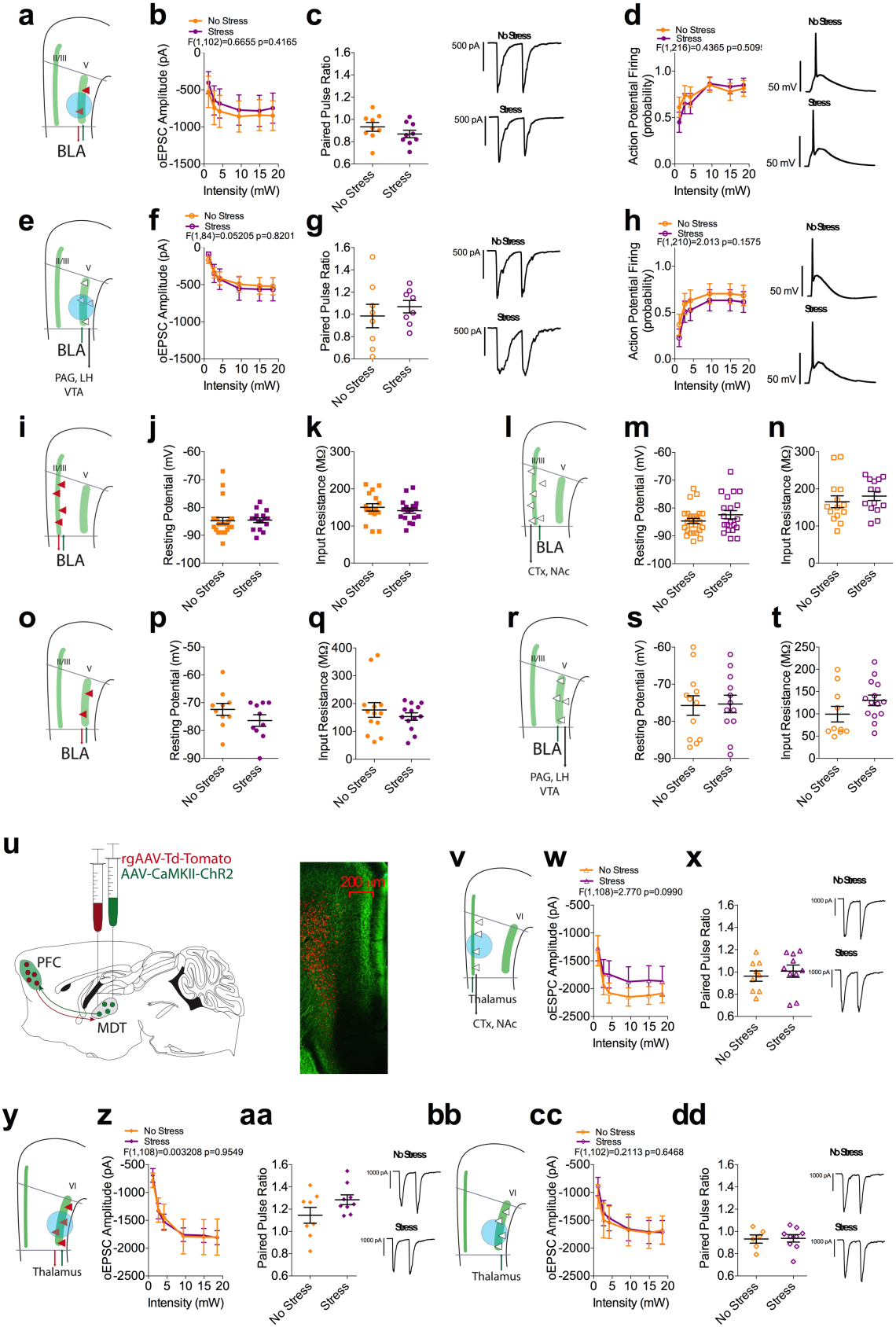
a
b
c
d
e
f
g
h
i
j
k
l
m
n
o
p
q
r
s
t
u
v
w
x
y
z
aa
bb
cc
dd
II/III
V
VI
BLA
PAG, LH
VTA
CTx, NAc
Thalamus
PFC
MDT
rgAAV-Td-Tomato
AAV-CaMKII-ChR2
200 µm
No Stress
Stress
F(1,102)=0.6655 p=0.4165
F(1,216)=0.4365 p=0.5095
F(1,84)=0.05205 p=0.8201
F(1,210)=2.013 p=0.1575
F(1,108)=2.770 p=0.0990
F(1,108)=0.003208 p=0.9549
F(1,102)=0.2113 p=0.6468
oEPSC Amplitude (pA)
Intensity (mW)
Paired Pulse Ratio
Action Potential Firing (probability)
500 pA
50 mV
1000 pA
Resting Potential (mV)
Input Resistance (MΩ)

Figure S2, related to figure 2: Stress does not alter excitatory input from the BLA to plPFC L5 neurons

(a) Schematic for voltage clamp-recordings of oEPSCs from L5 rAAV+ neurons at -70mV.
(b) Optically evoked input/output curve from L5 rAAV+ neurons from non-stressed (n=9, N=4) and stressed mice (n=10, N=4). Stress does not alter excitatory input from the BLA to plPFC L5 rAAV+ neurons.
(c) Effect of stress on paired pulse ratio (PPR) at BLA-L5 rAAV+ synapses (No Stress n=10, N=4; Stress n=9, N=4). Stress exposure does not alter PPR at BLA-L5 rAAV+ synapses (p=0.2413).
(d) Optically evoked spiking in L5 rAAV+ neurons in non-stressed (n=18, N=8) and stressed mice (n=20, N=8). Stress exposure does not alter optically evoked spiking in L5 rAAV+ neurons.
(e) Schematic for voltage clamp-recordings of oEPSCs from L5 rAAV- neurons at -70mV.
(f) Optically evoked input/output curve from L5 rAAV- neurons from non-stressed (n=8, N=4) and stressed (n=8, N=5) mice. Stress does not alter excitatory input onto L5 rAAV- neurons.
(g) Effect of stress on PPR at BLA-L5 rAAV- synapses (No Stress: n=8, N=5; Stress: n=8, N=4). Stress exposure does not alter PPR at BLA-L5 rAAV- synapses (p=0.4958).
(h) Optically evoked spiking in L5 rAAV- neurons in non-stressed (n=18, N=8) and stressed mice (n=19, N=7). Stress exposure does not alter optically evoked spiking in L5 rAAV- neurons.
(i) Schematic for current-clamp recordings from L2/3 rAAV+ neurons
(j) Resting membrane potential (RMP) of L2/3 rAAV+ neurons from non-stressed (n=24, N=10) and stressed (n=20, N=8) mice. Stress does not alter RMP in L2 rAAV positive neurons (p=0.8866).
(k) Input resistance (IR) of L2/e rAAV+ neurons from non-stressed (n=16, N=6) and stressed (n=17, N=5) mice. Stress does not alter IR in L2/3 rAAV+ neurons (p=0.4725).
(l) Schematic for current-clamp recordings from L2/3 rAAV- neurons
(m) RMP of L2/3 rAAV- neurons from non-stressed (n=26, N=8) and stressed (n=23, n=7) mice. Stress does not alter RMP in L2/3 rAAV- neurons (p=0.1852)
(n) IR of L2/3 rAAV- neurons from non-stressed (n=14, N=6) and stressed (n=15, N=6) mice. Stress does not alter IR in L2/3 rAAV- neurons (p=0.4494).
(o) Schematic for current clamp-recordings from L5 rAAV+ neurons at -70mV.
(p) RMP of L5 rAAV+ neurons from non-stressed (n=10, N=5) and stressed (n=10, N=3) mice. Stress does not alter RMP in L5 rAAV+ neurons (p=0.2014).
(q) IR of L5 rAAV+ neurons from non-stressed (n=12, N=6) and stressed (n=13, N=4) mice. Stress does not alter IR in L5 rAAV+ neurons (p=0.4312).
(r) Schematic for current-clamp recordings of oEPSCs from L5 rAAV- neurons
(s) RMP of L5 rAAV+ neurons from non-stressed (n=12, N=5) and stressed (n=12, N=5). Stress does not alter RMP in L5 rAAV- neurons (p=0.9073).
(t) IR of L5 rAAV- neurons from non-stressed (n=10, N=6) and stressed (n=14, N=5) mice. Stress does not alter IR in L5 rAAV- neurons (p=0.1415).
(u) Schematic for stereotaxic delivery of AAV5-CaMKII-ChR2(H147R)-eYFP and rAAV2-CAG-tdTomato into the MDT
(v) Schematic for voltage clamp-recordings of oEPSCs from L6 rAAV+ neurons at -70mV.

(w) Optically evoked input/output curve from L6 rAAV+ neurons from non-stressed (n=10, N=3) and stressed mice (n=10, N=3). Stress does not alter excitatory input to L6 rAAV+ neurons.
(x) Effect of stress on PPR at MDT-L6 rAAV- positive synapses (No Stress: n=8, N=3; Stress: n=9 N=3). Stress exposure does not alter PPR at MDT-L6 rAAV+ synapses (p=0.1075).
(y) Schematic for voltage clamp recordings of oEPSCs from L6 rAAV- neurons at -70mV.
(z) Optically evoked input output curve from L6 rAAV- neurons from non-stressed (n=9, N=3) and stressed mice (n=10, N=3). Stress does not alter excitatory input from the MDT to L6 rAAV- neurons.
(aa) Effect of stress on PPR at MDT-L6 rAAV- synapses (No Stress n=6, N=3; Stress: n=9, N=3). Stress exposure does not alter PPR at MDT-L6 rAAV- synapses (p=0.9048).
(bb) Schematic for voltage clamp recordings of oEPSCs from L2/3 rAAV- neurons at -70mV.
(cc) Optically evoked input output curve from L2/3 rAAV- neurons from non-stressed (n=9, N=3) and stressed (n=11, N=3) mice. Stress does not alter excitatory input to L2/3 rAAV- neurons.
(dd) Effect of stress on PPR at MDT-L2/3 rAAV- synapses (No Stress: n=9, N=3; Stress: n=10 N=3). Stress exposure does not alter PPR at MDT-L2/3 rAAV- synapses (p=0.5496).

All error bars represent ± SEM. “n” represents number of neurons, “N” represents number of mice. P values reported from two-tailed unpaired t-test (c,g,j,k,m,n,p,q,s,t,x,aa,dd). F and P values from ANOVA shown in relevant panels.

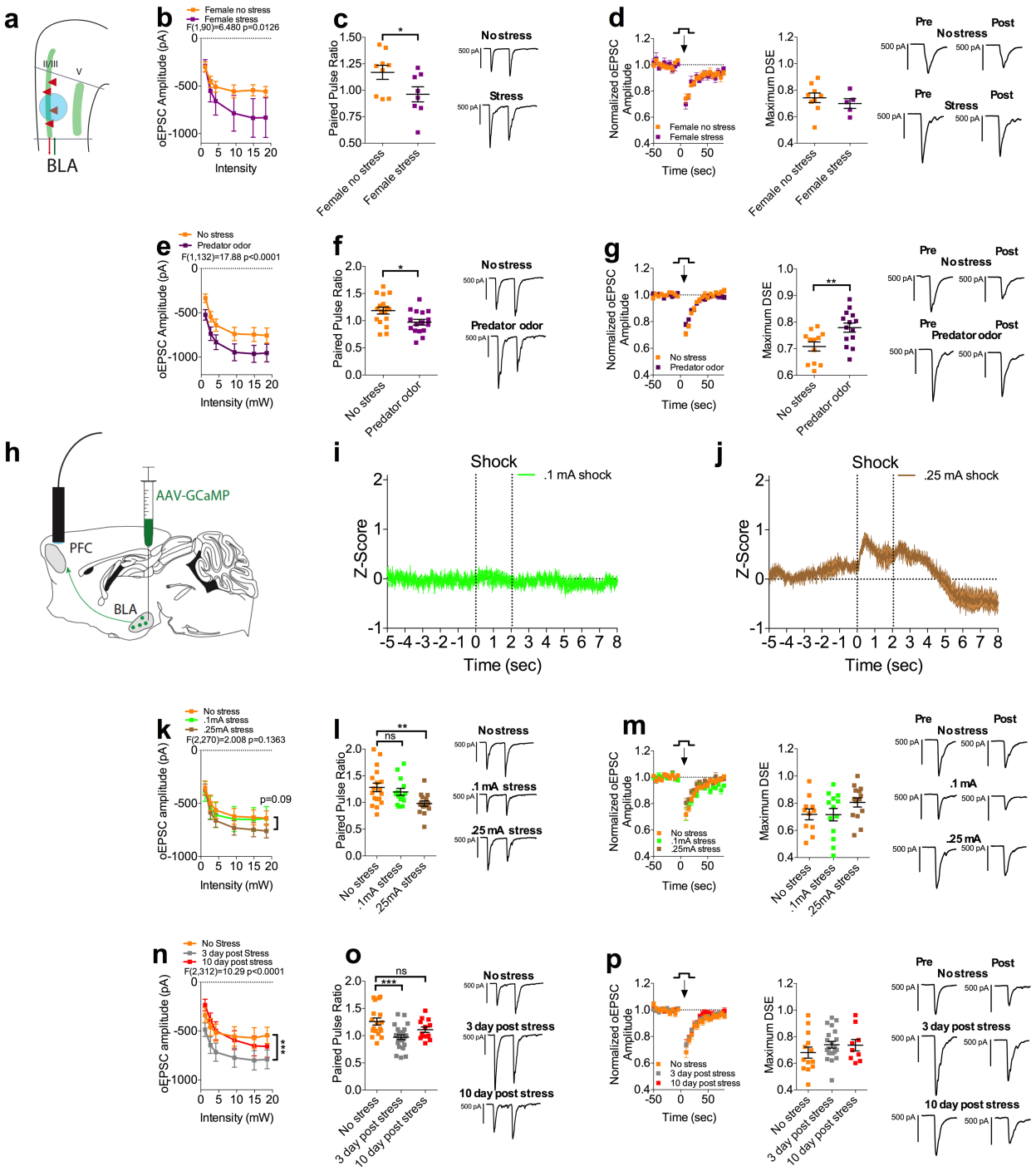

Figure S3, related to figure 2: Dose response, time course, and generalizability of stress induced presynaptic strengthening at BLA-L2 rAAV positive synapses

(a) Schematic for voltage-clamp recordings of oEPSCs from L2/3 rAAV+ neurons.

(b) Optically-evoked input/output curve from L2/3 rAAV+ neurons from non-stressed (n=9; N=3) and stressed (n=8; N=3 mice) female mice. Stress exposure enhances excitatory input to L2/3 rAAV+ neurons.

(c) Effect of stress on PPR at BLA-L2/3 rAAV+ synapses (No Stress: n=9, N=3, Stress: n=8, N=3). Stress exposure decreases PPR (p=0.0499).
(d) Effect of stress on DSE in female mice (No stress: n=9, N=3; Stress: n=5, N=3). Stress does not alter DSE magnitude in female mice (p=0.4560)
(e) Optically-evoked input/output curve from L2/3 rAAV+ neurons from mice receiving no stress (n=17, N=4) or 10 minutes exposure to the predator odorant, 2MT (n=16, N=4). Predator odor exposure significantly increases excitatory input to L2/3 rAAV+ neurons.
(f) Effect of predator odor on PPR at BLA-L2/3 rAAV+ synapses (No stress: n=16, N=4; Predator odor: n=17, N=4). Predator odor decreases PPR (p=0.0152).
(g) Effect of predator odor on DSE at BLA-L2/3 rAAV+ synapses (No stress: n=12, N=4; Stress: n=13, N=4). Stress decreases DSE magnitude (p=0.0078).
(h) Schematic for *in vivo* fiber photometry recordings of BLA projections to the plPFC
(i) Z-score of ΔF/F signal recorded from GCaMP6s expressing BLA terminals in the plPFC in response to 2 second 0.1 mA foot shock (N=5 mice, averaged from 20 shocks per mouse).
(j) Z-score of ΔF/F signal recorded from GCaMP6s expressing BLA terminals in the plPFC in response to 2 second 0.25 mA foot shock (N=5, averaged from 20 shocks per mouse).
(k) Optically-evoked input/output curve from L2/3 rAAV+ neurons from mice receiving no stress (n=19; N=4), 0.1 mA foot-shock stress (n=14; N=4), and 0.25 mA foot-shock stress (n=15, N=4). 0.25 mA stress exposure induces a trend toward increased excitatory input to L2/3 rAAV+ neurons (p=0.0943).
(l) Effect of 0.1 and 0.25 mA foot-shock stress on PPR at BLA-L2/3 rAAV+ synapses (No Stress: n=19, N=4, 0.1 mA stress: n=14, N=4, 0.25 mA stress: n=15, N=4). 0.25 mA stress exposure decreases PPR (p=0.0058).
(m) Effect of 0.1 and 0.25 mA foot-shock stress on DSE at BLA-L2/3 rAAV+ synapses (No stress: n=11, N=4; 0.1 mA stress: n=13, N=4; 0.25 mA stress: n=14, N=4). Neither 0.1 mA (p=0.9697) nor 0.25 mA (p=0.2504) foot-shock stress alter DSE magnitude.
(n) Optically-evoked input/output curve from L2/3 rAAV+ neurons from mice receiving no stress (n=18, N=4), and mice recorded 3 (n=24, N=4) and 10 days (n=13, N=4) following 0.5 mA foot shock stress. Stress exposure increases excitatory input to L2/3 rAAV+ neurons at 3 days post exposure (p=0.0002)
(o) Effect of 0.5 mA stress on PPR at BLA-L2/3 rAAV+ synapses at 3 and 10 days post exposure (no stress: n=18, N=4; 3 day: n=24, N=4; 10 day: n=13, N=4). PPR is decreased at 3 days post stress exposure (p=0.0003).
(p) Effect of 0.5 mA stress on DSE at BLA-L2/3 rAAV+ synapses at 3 and 10 days post exposure (no stress: n=13, N=4; 3 day: n=21, N=4; 10 day: n=9, N=4). DSE magnitude is not altered at 3 (p=0.3689) or 10 (p=0.3689) days post stress exposure.

All error bars represent ± SEM. “n” represents number of neurons, “N” represents number of mice. P values reported from two-tailed unpaired t-test (c,d,f,g) and one-way ANOVA (l,m,o,p). F and P values from ANOVA shown in relevant panels.

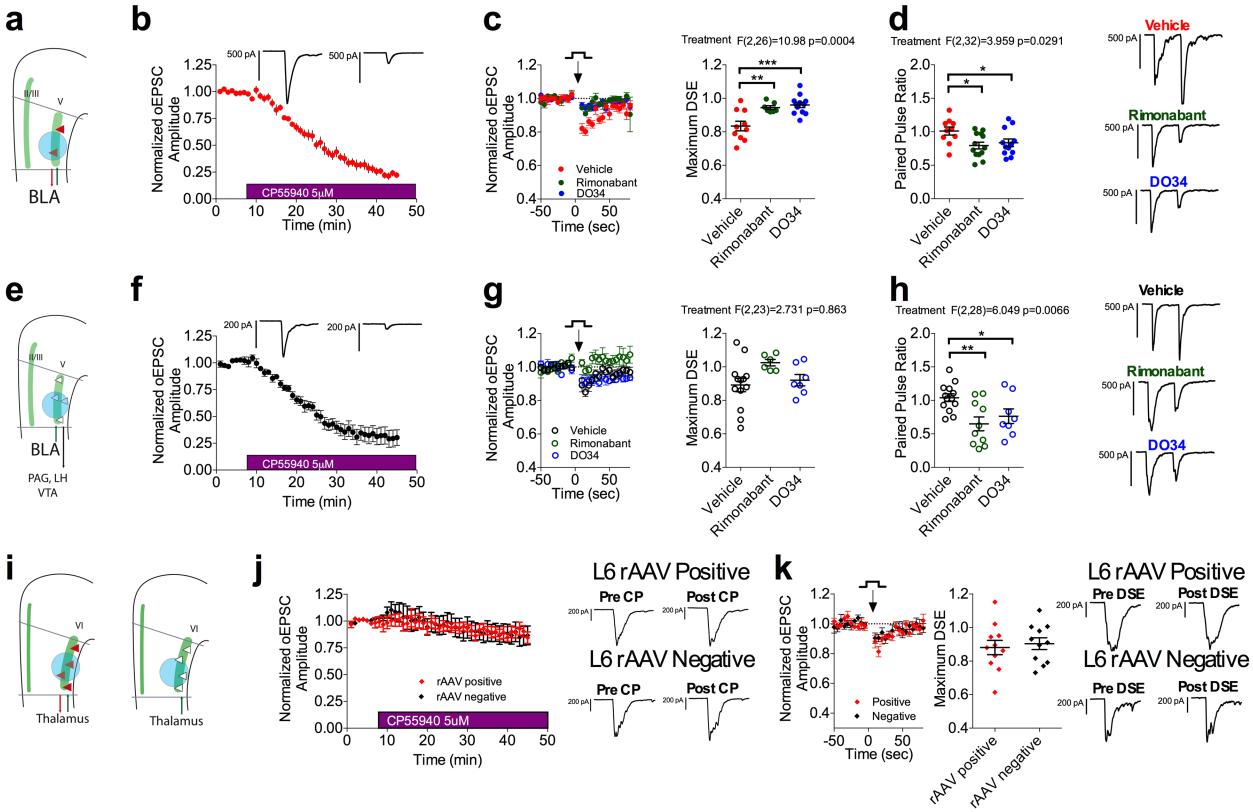

Figure S4, related to figure 3: Phasic and tonic 2-AG signaling broadly regulate BLA-plPFC L5 glutamatergic synapses but not MDT-plPFC synapses

(a) Schematic for voltage-clamp recordings of oEPSCs from L5 rAAV+ neurons at -70mV.

(b) Effect of 5 μM CP55,940 on oEPSC amplitude at BLA-L5 rAAV+ synapses (n=8, N=6).

(c) Depolarization induced suppression of excitation (DSE) at BLA-L5 rAAV+ synapses (n=11, N=5) is blocked by 10 μM rimonabant (n=7, N=4; One-way ANOVA with Holm-Sidak post-hoc correction, p=0.0023) and 2.5 μM DO34 (n=12, N=4; p=0.0003).

(d) PPR at BLA-L5 rAAV+ synapses (n=10, N=5) is reduced by rimonabant (n=13, N=4; p=0.0217) and DO34 (n=10, N=4; p=0.0389).

(e) Schematic for voltage clamp-recordings of oEPSCs from L5 rAAV- neurons at -70mV.

(f) Effect of CP55,940 on oEPSC amplitude at BLA-L5 rAAV- synapses (n=7, N=5)

(g) Minimal depolarization induced suppression of excitation (DSE) is evoked at BLA-L5 rAAV- synapses (n=13, N=5). As such, there is no significant effect of rimonabant (n=6, N=6; One-way p=0.0580) or DO34 (n=7, N=4; p=0.6040)

(h) PPR at BLA-L5 rAAV- synapses (n=13, N=5) is reduced by rimonabant (n=12, N=5; p=0.0047) and DO34 (n=8 N=4; p=0.0347).

(i) Schematic for voltage-clamp recordings of oEPSCs from L6 rAAV+ and negative neurons at -70mV.

(j) Effect of CP55,940 on oEPSC amplitude at MDT-L6 rAAV+ (n=8, N=6) and negative (n=10, N=6) synapses. CP55,940 does not induce significant depression of oEPSC amplitude at MDT-L6 rAAV+ or rAAV- synapses.

(k) Minimal DSE was evoked at MDT-L6 rAAV+ (n=11, N=3) and rAAV- (n=11, N=3) synapses.

All error bars represent ± SEM. "n" represents number of neurons, "N" represents number of mice. All post-hoc p values derived from one-way ANOVA with Holm-Sidak multiple comparisons (c,d,g,h) or two-tailed unpaired t-test (k). F and P values for ANOVA shown in relevant panels.

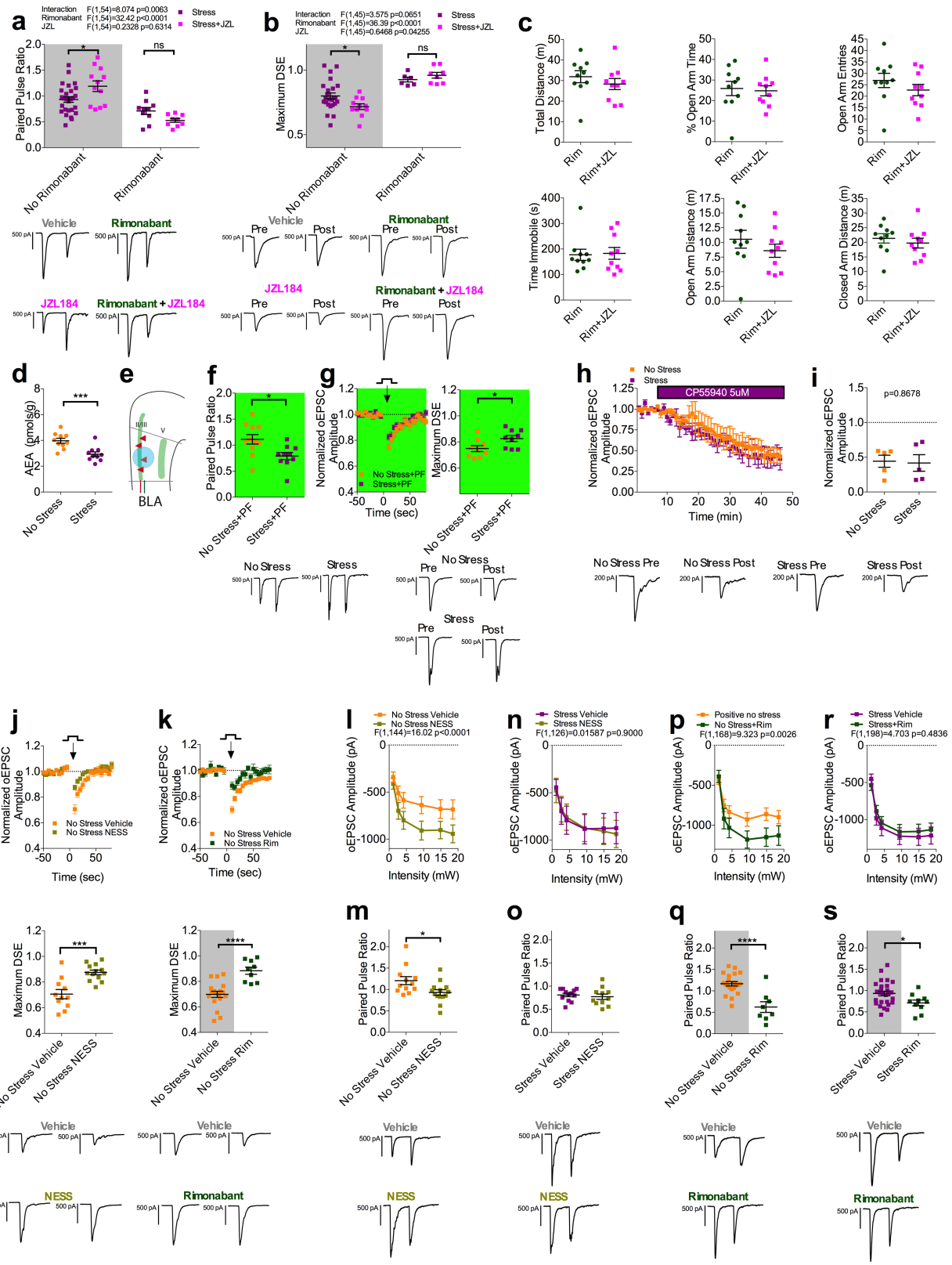
a
Interaction F(1,54)=8.074 p=0.0063
Rimonabant F(1,54)=32.42 p<0.0001
JZL F(1,54)=0.2328 p=0.6314
Stress
Stress+JZL
Paired Pulse Ratio
No Rimonabant
Rimonabant
Vehicle
Rimonabant
JZL184
Rimonabant + JZL184
b
Interaction F(1,45)=3.575 p=0.0651
Rimonabant F(1,45)=36.39 p<0.0001
JZL F(1,45)=0.6468 p=0.04255
Maximum DSE
Pre
Post
c
Total Distance (m)
% Open Arm Time
Open Arm Entries
Time Immobile (s)
Open Arm Distance (m)
Closed Arm Distance (m)
Rim
Rim+JZL
d
AEA (pmol/g)
No Stress
Stress
e
BLA
f
Paired Pulse Ratio
No Stress+PF
Stress+PF
g
Normalized oEPSC Amplitude
Maximum DSE
Time (sec)
h
No Stress
Stress
CP55940 5uM
Time (min)
No Stress Pre
No Stress Post
Stress Pre
Stress Post
i
p=0.8678
j
No Stress Vehicle
No Stress NESS
k
No Stress Rim
l
F(1,144)=16.02 p<0.0001
oEPSC Amplitude (pA)
Intensity (mW)
n
Stress Vehicle
Stress NESS
F(1,126)=0.01587 p=0.9000
p
Positive no stress
No Stress+Rim
F(1,168)=9.323 p=0.0026
r
Stress+Rim
F(1,198)=4.703 p=0.4836
m
o
q
s
NESS
Rimonabant

Figure S5, related to figure 4: Rimonabant blocks the effects of JZL184, AEA augmentation does not rescue stress-induced changes in PPR or DSE, stress does not alter CB1 sensitivity, and stress occludes the effects of NESS and rimonabant at BLA-L2/3 rAAV positive synapses

(a) Effect of JZL and JZL+rimonabant on PPR in stressed mice. 1 μM JZL reverses the stress-induced decrease in PPR at BLA-L2/3 rAAV+ synapses (Stress: n=27, N=11; Stress+JZL: n=13, N=4, Two-way ANOVA with Holm-Sidak post hoc correction, p=0.0158). JZL does not alter PPR in the presence of 10 μM rimonabant (Stress+rimonabant: n=10, N=5; Stress+rimonabant+JZL: n=9, N=2; p=0.1452). Stress and Stress+JZL without rimonabant from main text figure shown in grey shading.

(b) Effect of JZL and JZL+rimonabant on PPR in stressed mice. JZL reverses the stress-induced attenuation of DSE magnitude at BLA-L2/3 rAAV+ synapses (Stress: n=24, N=11; Stress+JZL: n=11, N=4). JZL does not alter DSE magnitude in the presence of rimonabant (p=0.5157). Stress and Stress+JZL without rimonabant from main text figure shown in grey shading.

(c) Effect of JZL in the presence of rimonabant in the EZM 24 hours after .5 mA foot-shock stress exposure. JZL has no behavioral effect in the presence of rimonabant. (Total Distance: p=0.3809)(Open Arm Time: p=0.7914)(Open Arm Entries: p=0.3042)(Time Immobile: p=0.8655)(Open Arm Distance: p=0.3127)(Closed Arm Distance: p=0.4981).

(d) Effect of stress on mPFC AEA levels. Stress exposure causes a decrease in mPFC AEA levels (No stress: N=10, Stress: N=10; p=0.0009).

(e) Schematic for voltage clamp-recordings of oEPSCs from L2 rAAV+ neurons at -70mV.

(f) Effect of 10 μM PF3845 on PPR at BLA-L2 rAAV+ synapses. PF3845 does not rescue the stress induced decrease in PPR at BLA-L2/3 rAAV positive synapses (No Stress: n=11, N=8; Stress: n=10, N=6; p=0.0121).

(g) Effect of PF3845 on DSE at BLA-L2 rAAV+ synapses. PF3845 does not rescue the stress induced decrease in DSE magnitude at BLA-L2/3 rAAV positive synapses (No Stress: n=9, N=6; Stress: n=9, N=6; p=0.0299).

(h) Effect of 5 μM CP55,940 on oEPSC amplitude at BLA-L2/3 rAAV+ synapses.

(i) Quantification of last 5 minutes of CP55,940 application on oEPSC amplitude at BLA-L2 rAAV+ synapses. Stress does not cause a significant change in CP55,940 induced depression of oEPSC amplitude at BLA-L2/3 rAAV+ synapses (No Stress: n=5, N=3; Stress: n=5, N=2; p=0.8678).

(j) Effect of 1 μM NESS on DSE at BLA-L2/3 rAAV+ synapses in non-stressed mice (vehicle: n=11, N=4; NESS: n=13, N=4). NESS blocks DSE (p=0.0002).

(k) Effect of 10 μM rimonabant on DSE at BLA-L2/3 rAAV+ synapses in non-stressed mice (vehicle: n=18, N=7; NESS: n=9, N=4). Rimonabant blocks DSE (p<0.0001). Grey shading: No Stress Vehicle data taken from main text.

(l) Effect of NESS on optically-evoked input/output curve from L2/3 rAAV+ neurons from non-stressed mice (vehicle: n=12, N=4; NESS: n=14, N=4). NESS enhances excitatory input.

(m) Effect of NESS on PPR at BLA-L2/3 rAAV+ synapses from non-stressed mice (vehicle: n=12, N=4; NESS: n=14, N=4). NESS decreases the PPR (p=0.0209).

(n) Effect of NESS on optically-evoked input/output curve from L2/3 rAAV+ neurons from stressed mice (vehicle: n=12, N=4; NESS: n=11, N=4). NESS does not affect excitatory input following stress.

(o) Effect of NESS on PPR at BLA-L2/3 rAAV+ synapses from stressed mice (vehicle: n=12, N=4; NESS: n=11, N=4). NESS does not affect PPR following stress ($p=0.5873$).
(p) Effect of rimonabant on optically-evoked input/output curve from L2/3 rAAV+ neurons from non-stressed mice (vehicle: n=21, N=8, rimonabant: n=8, N=4). Rimonabant enhances excitatory input.
(q) Effect of rimonabant on PPR at BLA-L2/3 rAAV+ synapses from non-stressed mice (vehicle: n=21, N=8, rimonabant: n=8, N=4). Rimonabant decreases the PPR ($p<0.0001$).
(r) Effect of rimonabant on optically-evoked input/output curve from L2/3 rAAV+ neurons from stressed mice (vehicle: n=27, N=10; rimonabant: n=10, N=4). Rimonabant does not affect excitatory input following stress.
(s) Effect of rimonabant on PPR at BLA-L2/3 rAAV+ synapses from stressed mice (vehicle: n=27, N=10; rimonabant: n=10, N=4). Rimonabant decreases the PPR following stress ($p=0.0297$).

All error bars represent ± SEM. "n" represents number of neurons, "N" represents number of mice. P values reported from two-tailed unpaired t-test (c,d,f,g,i,j,k,m,o,q,s) and post-hoc p values reported from two-way ANOVA with Holm-Sidak multiple comparisons (a,b). F and P values for ANOVA shown in relevant panels.

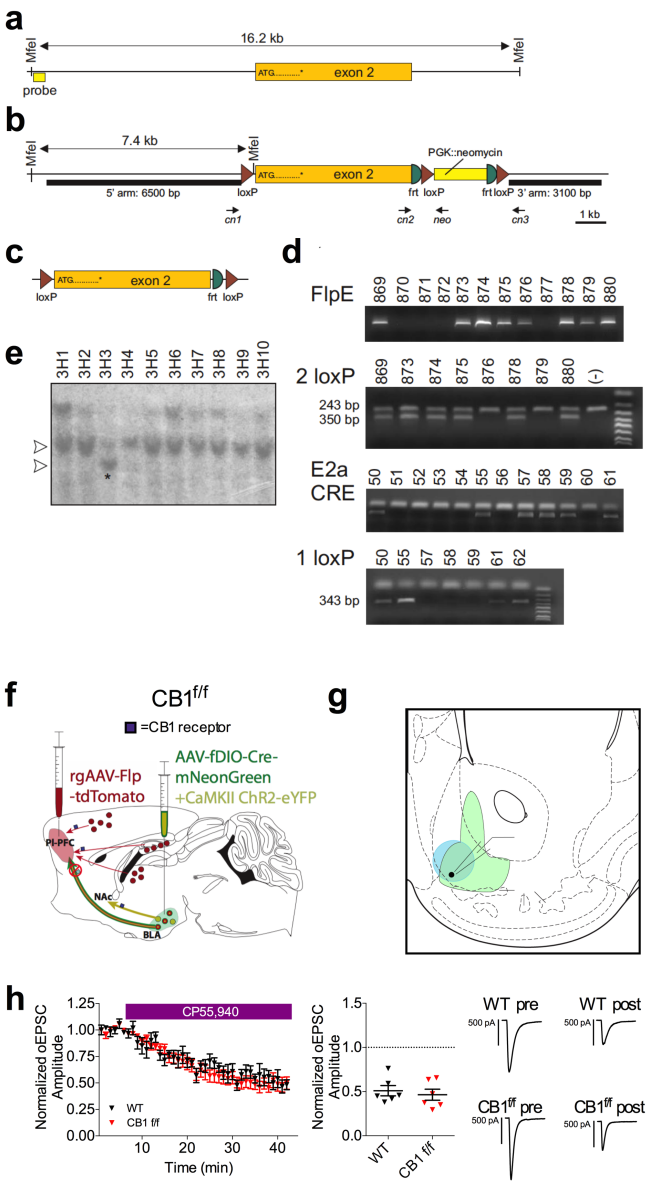

Figure S6, related to figure 6: INTRSECT approach leads to selective deletion of the CB1 receptor from BLA neurons that project to the plPFC and not from BLA neurons that project to other brain regions

(a) Schematic representation of the *Cnr1* gene with exons 1 and 2 separated by large intron.

(b) Schematic representation of the *Cnr1* gene after homologous recombination. Three loxP and 2 FRT sites are highlighted around the coding exon. A PGK-driven neomycin resistance gene cassette is also included. The 5' and 3' arms of recombination are also highlighted. Note the location of PCR primers used to genotype the mice: Primers cn2 – neo were used to amplify a 389 bp fragment from the mutant allele only; primers cn2 and cn3 amplify a 342 and 350 bp fragments from wild-type allele and 2 loxP allele, respectively; primers cn1 and cn3 amplify a 343 bp fragment once exon 2 has been deleted.

(c) Structure of the mutant allele after FlpE-mediated recombination. This recombination eliminates the neomycin cassette and leaves exon 2 flanked by 2 loxP sites.
(d) Southern blot analysis of 10 ES cell clones showing the presence of a 16 kb band in all samples and a smaller 7.4 kb fragment in clone 3H3.
(e) PCR analysis of progeny of 3 loxP mice crossed with FlpE mice giving rise to mice demonstrating a 350 bp fragment originating from the 2 loxP allele. Also shown is a PCR analysis of progeny of 2 loxP mice crossed with E2a-CRE mice giving rise to mice demonstrating a 343 bp fragment originating from the 1 loxP allele.
(f) Schematic for deletion of CB1 from plPFC projecting BLA neurons and expression of CaMKII-ChR2-eYFP in BLA projection neurons.
(g) Schematic for recording of BLA evoked oEPSCs in the Nucleus Accumbens (NAc) Shell
(h) Effect of CP55,940 on oEPSC amplitude at BLA-NAc shell synapses. WT and $CB1^{f/f}$ INTRSECT mice have equal sensitivity to CP55,940 induced depression of BLA evoked oEPSCs in the NAc shell (WT: n=6, N=3; $CB1^{f/f}$ n=6, N=2; p=0.6048).

All error bars represent ± SEM. "n" represents number of neurons, "N" represents number of mice. P values reported from two-tailed unpaired t-test (h).